A novel camptothecin derivative, ZBH-01, exhibits superior antitumor efficacy than irinotecan by regulating the cell cycle

Yongqi Li
Jilin University
Dawei Zhao
Jilin Cancer Hospital
Wenqiu Zhang
Jilin University
Miaomiao Yang
Jilin University
Zhihui Wu
Jilin University
Weiguo Shi
Beijing Institute of Pharmacology and Toxicology: Academy of Military Medical Sciences Institute of Pharmacology and Toxicology
Shijie Lan
Jilin University
Zhen Guo
Jilin University
Hong Yu
Jilin Cancer Hospital
Di Wu (wudi1971@jlu.edu.cn)
The First Hospital of Jilin University: Bethune First Hospital of Jilin University https://orcid.org/0000-0002-0742-0556

Research Article

Keywords: irinotecan derivative ZBH-01, colorectal cancer, next-generation sequencing, differentially expressed genes, cell cycle, apoptosis

Posted Date: July 27th, 2022

DOI: https://doi.org/10.21203/rs.3.rs-1770908/v1

Version of Record: A version of this preprint was published at Journal of Translational Medicine on June 29th, 2023. See the published version at https://doi.org/10.1186/s12967-023-04196-2.

Abstract

Irinotecan (CPT-11) is a classic chemotherapeutic agent that plays an important role in the clinical treatment of metastatic colon cancer and other malignant tumors. We previously designed a series of novel irinotecan derivatives and selected one representative, ZBH-01, to investigate its sophisticated antitumor mechanisms in colon tumor cells. Our current results showed that ZBH-01 has superior antitumor activity against colon cancer cells compared to CPT-11 and SN38 (7-Ethyl-10-hydroxy camptothecin), both *in vivo* and *in vitro*. However, its inhibitory ability on topoisomerase I (TOP1) was weaker than these two control drugs. Moreover, 842 mRNAs were downregulated and 927 were upregulated in the ZBH-01-treated group by Next-Generation Sequencing (NGS) and bioinformatics analysis. The most significantly enriched KEGG pathways for these dysregulated mRNAs were DNA replication, the p53 signaling pathway, and the cell cycle. Then, we constructed a protein-protein interaction (PPI) network and identified a significant cluster containing 73 genes, including 14 involved in the cell cycle process. ZBH-01 induced G_0/G_1 phase arrest and enhanced the levels of p53 protein in colon cancer cells, while CPT-11/SN38 caused S phase arrest. The initiation of apoptosis by ZBH-01 was also superior to CPT-11/SN38, followed by the increased expression of Bax, active caspase 3, and cleaved-PARP, and decreased expression of Bcl-2. Additionally, CCNA2 (cyclin A2), CDK2 (cyclin-dependent kinase 2), and MYBL2 (MYB proto-oncogene like 2) might be involved in the G_0/G_1 cell cycle arrest induced by ZBH-01. Overall, ZBH-01 can be an antitumor candidate drug for preclinical study in the future.

1. Introduction

Colorectal cancer (CRC) is one of the main five cancer types and the five most common causes of cancer-related deaths in China [1]. According to the 2015 Chinese Cancer Statistics, the incidence and mortality of CRC in both males and females are continuously increasing [2]. Despite significant progress in precision medicine, CPT-11 remains the primary chemotherapeutic agent for the treatment of metastatic CRC [3, 4].

CPT-11 is a camptothecin (CPT) analog, which was discovered from plant extracts more than 60 years ago. It disturbs the catalytic cycle of DNA TOP1 by stabilizing the reversible covalent enzyme-DNA cleavable complex. Moreover, by forming a drug-enzyme-DNA ternary complex during DNA synthesis, CPT-11 triggers the formation of irreversible single-stranded DNA break when the cleavable complex collides with the DNA replication fork [5]. This specific cytotoxic effect characterizes CPT-11 as a potent antitumor agent. However, its poor water solubility and serious side effects hinder its clinical applications. Until now, only two CPT analogs (irinotecan and topotecan) have been approved for cancer treatment worldwide [6]. Although a large number of CPT derivatives have been synthesized and actively studied, their results were unsatisfactory [7, 8]. Thus, a breakthrough in the development of novel CPT analogs is still an urgent problem to be solved.

In the last ten years, our research group designed and synthesized a series of novel irinotecan derivatives characterized by higher antitumor activity for tumor cells and lower toxicity for epithelial cells compared to CPT-11 [9-11]. However, the molecular mechanisms of these new derivatives still need to be precisely elucidated. Therefore, in the present study, we explored the antitumor mechanisms of one representative compound, ZBH-01, that showed a higher inhibitory effect on the development of colon tumors than irinotecan in our preliminary experiments.

2. Materials And Methods

2.1 Agents

ZBH-01 was synthesized by the Institute of Pharmacology and Toxicology Academy of Military Medical Sciences (China), the chemical structure of ZBH-01 is shown in Fig. 1A. CPT-11 and SN38 (the activated form of irinotecan) were provided by the same institution. All chemical agents were dissolved in dimethyl sulfoxide (DMSO; Sigma-Aldrich, St. Louis, MO, USA) and stored at -80°C before use.

2.2 Cell lines

Thirteen human tumor cell lines, a normal human colon mucosal epithelial cell lines (HcoEpic), and the HEK293 cell lines were maintained in DMDM or RPMI 1640 media (Life Technologies, Grand Island, NY, USA) supplemented with 10% fetal bovine serum (FBS, Gibco), 2 mmol/L glutamine, 100 U/mL penicillin, and 100 μg/mL streptomycin in a humidified incubator at 37°C and 5% CO_2.

2.3 Cell viability assay in vitro

The cytotoxic activity of ZBH-01 was evaluated against the above cell lines using MTT or Cell Counting Kit-8 (CCK8) assay as previously described [9, 11]. HEK293 and HcoEpic cells were used as control cells. The different cell lines, including the colon cancer cell lines, were treated with different concentrations of ZBH-01, CPT-11, and SN38. After 72 h of incubation, the absorbance of cells in each group was measured at 450 nm using a spectrophotometer. The IC_{50} values (50% inhibition of cell growth) were calculated by SPSS (Statistical Product and Service Solutions) 23.0.

2.4 DNA relaxation assay

The DNA relaxation assay was performed according to the manufacturer's instructions (TopoGEN, Inc., Port Orange, FL, USA) [11]. The reaction was conducted in a dosage-dependent manner. We also performed qRT-PCR and Western blot to evaluate the inhibition of ZBH-01 on TOP1 in LS174T or SW1116 colon cancer cells. The primers of TOP1 (DHS626257) were provided by XYbiotech (Shanghai, China). The forward (5'-CTACCTCATGAAGATCCTCACCGA-3') and reverse (5'-TTCTCCTTAATGTCACGCACGATT-3') primers of β-actin were provided by Shanghai Generay Biotech Co., Ltd. Total RNA isolation, first-strand cDNA synthesis, and the qRT-PCR assay was performed as described below (see qRT-PCR assay section) [12].

2.5 NGS (Next-Generation Sequencing)

First, LS174T cells were subjected to 50 nmol/L ZBH-01, CPT-11, and SN38 for 24 h. Total RNA was extracted using TRIzol reagent (Invitrogen, CA, USA) following the manufacturer's instructions. Total RNA quantity and purity were analyzed by Bioanalyzer 2100 and RNA 6000 Nano Lab Chip Kit (Agilent, CA, USA) with RIN number > 7.0. Then, 3 μg RNA per sample was used to prepare RNA-Seq libraries. Sequencing libraries were generated using NEBNext Ultra II RNA Library Prep Kit for Illumina (NEB, E7760) following the manufacturer's recommendations. The PCR was performed with Phusion High-Fidelity DNA polymerase, universal PCR primers, and index (X) Primer. Finally, PCR products were purified (AMPure XP system) and library quality was assessed on the Agilent Bioanalyzer 2100 system. Paired-end sequencing was performed using Illumina HiSeq X Ten (Illumina, San Diego, CA). Raw data (raw reads) in the fastq format were processed by the Fastp software. All downstream analyses were based on clean high-quality data. Paired-end clean reads were aligned to the reference genome using STAR V20201. Cufflinks v2.2.1 was used to count the number of reads mapped to each gene. The FPKM of each gene was calculated based on the length of the gene and the count of reads mapped to this gene. The resulting *p*-values were adjusted using Benjamini and Hochberg's approach for controlling the false discovery rate (FDR).

2.6 Differential expression analysis of mRNAs

To compare mRNA expression differences among ZBH-01, CPT-11, and SN38 groups, a p-value < 0.05 and $|\log_2$ fold change$| > 1$ were set as the threshold for significantly differential expressions. First, the gene expression profiles of the three groups were compared to the control group. Then the three datasets obtained were analyzed together to obtain commonly expressed genes and a ZBH-01 group-specific differentially expressed gene list.

2.7 Bioinformatics analyses

Gene Ontology (GO) classifications (biological process, cellular component, and molecular function) and the Kyoto Encyclopedia of Genes and Genomes (KEGG) pathway enrichment analyses were hierarchically investigated using 'clusterProfiler' in R 3.4.0 (R Foundation, Vienna, Austria) [13] and KEGG Pathway Database (http://www.genome.jp/kegg/pathway.html). The proteins encoded by upregulated and downregulated differentially expressed mRNAs (DEmRNAs) in the ZBH-01 group were used to construct a PPI network using STRING (https://string-db.org/) and Cytoscape 3.5.1 (http://www.cytoscape.org/, The Cytoscape Consortium, San Diego, CA, USA) [14, 15]. We used Cytotype MCODE to identify key network modules and select hub genes.

2.8 qRT-PCR assay

The PCR primers of some genes are shown in Table 1. Besides, the primers of other genes were provided by XYbiotech (Shanghai, China) including BUB1 (catalog number. DHS322648), BUB1B (DHS646748), CCNA2 (DHS819739), CDC20 (DHS889533), CDC25C (DHS740393), CDC45 (DHS793726), CDC7 (DHS095090), CDK2 (DHS278875), CHEK1 (DHS670983), E2F8 (DHS048256), EZF2 (DHS068552), FOXM1 (DHS718140), MCM3 (DHS061267), MCM7 (DHS794915), MYBL2 (DHS516386), ORC1 (DHS500377), PKMYT1 (DHS687810), RAD54L (DHS609809), TOP2A (DHS036498), and TTK (DHS713780). Total RNA isolation was performed with the EasyPure RNA kit (Transgen) according to the

manufacturer's guidelines. RNA concentrations were measured by a microplate reader (BioTek Synergy H1). The TransScript All-in-One First-Strand cDNA Synthesis SuperMix for qPCR kit was used for reverse transcription according to the manufacturer's instructions. The 20μL reaction volumes contained 1 μg RNA prepared by combining 4 μL transcript all-in-one supermix for qPCR, 1 μL gDNA remover, and variable RNase-free water. The reverse transcription reactions were performed for 15 min at 42°C and 5 s at 85°C. Each reverse transcription product was diluted 10 times by adding 180 μL H_2O to 20 μL cDNA. The qPCR with TransStart Tip Green qPCR SuperMix kit (Transgen) was also performed according to the manufacturer's protocol. Briefly, 20 μL reaction volume were prepared by combining 10 μL transstart tip green qPCR supermix, 0.4 μL passive reference dye, 0.5 μL forward primer and 0.5 μL reverse primer, 3 μL cDNA and 5.6 μL ddH_2O. The cycling conditions were: 94°C for 30 s, 40 cycles at 94°C for 5 s, and 60°C for 30 s. The relative gene expression data were analyzed by the $2^{-\triangle\triangle CT}$ method.

Table 1
Primers for qRT-PCR.

Genes	Forward primer (5’-3’)	Reverse primer (5’-3’)
MCL1	TCTCATTTCTTTTGGTGCCTTTG	TAACTAGCCAGTC(TGTTTTGTC
XIAP	GTGAATGCTCAGAAAGACAGTATGC	TGTCCACAAGGAACAAAAACGATAG
BIRC3	GATGCTGGATAACTGGAAAAGAG	TGAAGAAGGAAAAGTAGGCTGAG
MDMX	ATTTTCCTTTTCAGGTATGGC	AGGTACTGTTTTCGTTGTTGG
MDM2	AAGGGAAGAAACCCAAGACAAAGA	GCACATGTAAAGCAGGCCATAAGA
CYC	TGATGCCTTTGTTCTTATTGG	TTTATTATGAAGTGTTCCCAGTG
APAF-1	ATCTGGGCTTCTGATGAAACTGC	CAACACCCAAGAGTCCCAAACAT
CASP9	AGCCAACCCTAGAAAACCTTACC	TCACCAAATCCTCCAGAACCAAT
cBid	GTCACACGCCGTCCTTGCT	CTGTCCGTTCAGTCCATCCCATT
BAX	AGGATGCGTCCACCAAGAAGC	GGCAAAGTAGAAAAGGGCGACA
BCL-XL	GAGAATCACTAACCAGAGACGAGA	GGAGAGAAAGTCAACCACCAGC
PTEN	TAAGGACCAGAGACAAAAAGGGA	GGCAGACCACAAACTGAGGATT
CDK6	TGATCAACTAGGAAAAATCTTGGAC	GGCAACATCTCTAGGCCAGT
NEK2	TGTCTCTGGCAAGTAATCCAG	CAGGTCCTTGCACTTGGACT
CCND1	AGCTGTGCATCTACACCGAC	TGTGAGGCGGTAGTAGGACA
CCNE2	ACCTCATTATTCATTGCTTCCAA	TCTTCACTGCAAGCACCATC
BIRC5	TTCTCAGTGGGGCAGTGGATG	TTTCTCAAGGACCACCGCATCT
CDK4	CTTCTGCAGTCCACATATGCAACA	CAACTGGTCGGCTTCAGAGTTTC
P53	AGCTTTGAGGTGCGTGTTTGTG	TCTCCATCCAGTGGTTTCTTCTTTG
Genes	**Forward primer (5’-3’)**	**Reverse primer (5’-3’)**
RB1	CACAACCCAGCAGTTCAATATC	TGAGATCACCAGATCATCTTCC
ATM	TGTGACTTTTCAGGGGATTTG	ATAGGAATCAGGGCTTTTGGA
ATR	GGGAATCACGACTCGCTGAA	CTAGTAGCATAGCTCGACCATGGA
XAF1	GCCTACTTGCTGTGGTGGTCTTGT	ACGCCTGGTTTGTTGAGGGTTTT
P21	TTAAACAAAAACTAGGCGGTTGA	AGGAGAACACGGGATGAGGA
CASP3	TGGCATTGAGACAGACA	GGCACAAAGCGACTG

2.9 Flow cytometry

To analyze the changes in the cell cycle, cell apoptosis, and mitochondrial membrane potential (MMP), SW1116 and LS174T colon cancer cells were harvested after exposure to 50 nmol/L ZBH-01, CPT-11, and SN38 for 12–72 h. Then, cells were stained by FxCycle™ PI/RNase Staining Solution (Invitrogen), FITC Annexin V Apoptosis Detection kit I (BD Biosciences, San Diego, CA, USA), and Mitochondrial Membrane Potential Detection Kit (BD Biosciences, San Diego, CA, USA) according to the manufacturer's protocol. Flow cytometry was performed using a FACS Calibur system (BD Dickinson). A minimum of 10,000 events was recorded for each sample. Data were acquired and analyzed by CellQuest (BD Biosciences), ModFit 4.0 (BD Biosciences), and FlowJo (TreeStar, Inc., Ashland, OR) software [11].

2.10 Western blot

First, SW1116 and LS174T cells were seeded in 6-well plates with a complete medium as previously described [9]. After cultivation for 24 h, cells were treated with 50 nmol/L ZBH-01, CPT-11, and SN38 for 48 h and harvested. Next, cell pellets were lysed and the protein concentrations of each sample were measured. Then, samples were separated by 10% SDS-PAGE and transferred to a polyvinylidene difluoride membrane (GE Healthcare, Piscataway, NJ). Samples were incubated with corresponding primary antibodies (1:500–1000 dilution) in 5% BSA at 4°C overnight. Then, the membrane was washed and incubated with appropriate secondary antibodies at room temperature for 1 h. The antibodies included TOP1, caspase 3, PARP, P53, Bax, and Bcl-xL (54H6) (Cell Signaling Technology, Shanghai, China). β-actin was used as the internal reference (1:5000 dilution). Protein bands were visualized with ECLplus Western Blotting Detection Reagents (GE Healthcare) on the ECL System (Millipore, Billerica, MA) [11].

2.11 Antitumor activity of ZBH-01 in vivo

The antitumor activity *in vivo* was evaluated using 6–8 week-old female nude mice as previously described [10]. All animal experiments were performed according to the animal experimental guidelines of the Jilin University. Tumor cell line xenografts were established by subcutaneous injection of $5x10^6$ LS174T cells in the left flank. Tumors were measured with vernier calipers twice a week. When masses reached 100–150 mm^3, mice were randomly assigned to the treatment (n = 6) or control (n = 6, treated with saline) groups. Mice in the treatment group intravenously (i.v.) received ZBH-01 (40 mg/kg) or CPT-11 (40 mg/kg) using the q4dx3w schedule [16, 17]. Animals were treated for 21 d, monitored twice a week for signs of toxicity, and weighed every 3 d. At the end of treatment, tumor tissues were stripped and tumor volume and growth inhibition were calculated [18]. Tumor volume (TV) = length × $width^2$ /2; Relative tumor volume (RTV) = TV_t /TV_0 (TV_t: tumor volume at day t, TV_0: tumor volume at the initiation of treatment); Relative tumor proliferation (T/C) = RTV_t /RTV_C × 100% (RTV_t: the treatment group RTV, RTV_C: the control group RTV).

2.12 Statistical analyses

Data are expressed as means ± standard deviations (SDs). One-way analysis of variance (ANOVA), χ^2 test, the two-tailed Student's *t*-test, or Mann–Whitney *U* test was performed using SPSS 23.0 software (SPSS, Inc., Chicago, IL, USA) and GraphPad Prism version 8.01 (GraphPad Software, San Diego, CA, USA). A $p < 0.05$ was considered statistically significant.

3. Results

3.1 ZBH-01 showed superior antitumor effects than CPT-11 and SN38

CPT-11 is a prodrug and SN38 represents its metabolically-activated form in the body. Therefore, we used CPT-11 or SN38 as positive controls in our study. The capacity of ZBH-01 to inhibit cell proliferation was assessed against 13 human tumor cell lines. The IC_{50} results are presented in Fig. 1B. We observed that the IC_{50} values of ZBH-01 are significantly lower than those of CPT-11 and SN38 in most tumor cell lines, while comparable in normal epithelial cells. Thereforce, ZBH-01 showed comparable or higher inhibitory anti-proliferative effect as compare to CPT-11 or SN38.

3.2 The reduction of TOP1 activity by ZBH-01 is weaker compared to CPT-11 and SN38

By forming a drug–enzyme–DNA complex, the drug prevents the relegation step normally catalyzed by topoisomerase, finally inhibiting the relaxation activity. Hence, to explore the interaction of ZBH-01 and TOP1, we performed a DNA relaxation assay. The inhibitory effect of ZBH-01 on TOP1 was weaker than CPT-11 and SN38 (Fig. 2). This result was contradictory to our previous reports [9, 11], which might indicate the heterogeneity and complexity of ZBH-01 mechanisms. Nevertheless, after treatment with 50 nmol/L ZBH-01 for 24 h, LS174T cells presented decreased protein levels of TOP1 (Fig. 9), while its mRNA levels were not suppressed (Fig. 5). This result was consistent with previous studies, indicating a significant downregulation of TOP1 in tumor cells treated with topoisomerase inhibitors [17, 18]. The reasons for our conflicting results remain to be further elucidated.

3.3 ZBH-01 treatment leads to the highest number of DEmRNAs in LS174T cells compared to CPT-11 and SN38

Previous studies have identified hundreds of abnormally expressed protein-coding genes in tumor cells after treatment with various drugs [19, 20]. Additionally, the gene expression profile of colon cancer cells can be used to predict and distinguish the response to multiple chemotherapeutic agents [21]. Hence, we used NGS to analyze expression changes in LS174T cells in response to ZBH-01 treatment. After performing the t-test, we used $p < 0.05$ and $|\text{Log}_2$ fold change$| > 1$ as criteria to screen out 2072 DEmRNAs

(1026 downregulated and 1046 upregulated) between ZBH-01 and controls; 380 DEmRNAs (251 downregulated and 129 upregulated) between CPT-11 and the control group; and 377 DEmRNAs (215 downregulated and 162 upregulated) between SN38 and controls. The Venn diagrams were used to classify the DEmRNAs among ZBH-01, CPT-11, and SN38 groups (Fig. 3A,B). The three groups shared 100 DEmRNAs (62 downregulated and 38 upregulated mRNAs). Compared to CPT-11 and SN38, the ZBH-01-treated group presented 1769 DEmRNAs (842 downregulated and 927 upregulated mRNAs). These results suggested that ZBH-01 might have a unique anti-tumor mechanism.

3.4 Clustering of specific GO items and KEGG pathways in the ZBH-01-treated group

Next, we performed GO enrichment analysis using 1769 DEmRNAs specific to the ZBH-01 group. The DEmRNAs were classified regarding their molecular functions (MF), biological processes (BP), and cellular components (CC). For BP (Fig. 4A), the DEmRNAs were mainly enriched in sister chromatid segregation, DNA-dependent DNA replication, and chromosome segregation. For CC (Fig. 4B), the DEmRNAs were mainly enriched in the chromosomal region, condensed chromosome, and spindle. Regarding MF (Fig. 4C), the DEmRNAs were mainly enriched in catalytic activity, acting on DNA, DNA-dependent ATPase activity, and DNA-secondary structure binding. The KEGG pathway results revealed that most ZBH-01 group-specific DEmRNAs were clustered in DNA replication, p53 signaling pathway, and cell cycle (Fig. 4D).

3.5 The proteins encoded by DEmRNAs specific to the ZBH-01 group were prominently involved in cell cycle regulation

Further, we constructed a PPI network (Fig. 5A) based on the proteins encoded by ZBH-01 group-specific DEmRNAs using the STRING database (http://string-db.org) [22]. We filtered out one prominent module (score = 61.833) from the PPI network using Cytotype MCODE (Fig. 5B) [23]. This module consists of 73 downregulated genes. Then, we conducted enrichment analysis again with these 73 genes demonstrating that they were principally associated with cell cycle, progesterone-mediated oocyte maturation, and oocyte meiosis. Fourteen genes (CDC45, CDC20, BUB1, CCNA2, BUB1B, TTK, CHEK1, CDC25C, MCM3, MCM7, ORC1, CDK2, CDC7, and PKMYT1) were involved in the most enriched cell cycle pathway (Fig. 5C).

Interestingly, we found that TOP2A is in the center of the module. In the relaxation assay results, we observed that the inhibition of ZBH-01 on TOP1 was weaker than CPT-11 and SN38. Thus, we need to further explore whether TOP2A is also a target of ZBH-01. Other key genes were also included in the module, such as FOXM1, RAD54L, UHRF1, MYBL2, EZH2, and E2F8, and play important roles in regulating the cell cycle.

3.6 Relative expression of some ZBH-01 group-specific DEmRNAs by qRT-PCR

Next, we selected some genes in Fig. 5B to perform qRT-PCR. These genes included not only the aforementioned DEmRNAs, but also classical genes involved in the cell cycle, DNA replication, and apoptosis regulation because they play important roles in CPT-11 anti-tumor process as reported by our group and others [3, 6, 9, 11, 20]. The results demonstrated that the expression trend of most genes was consistent with the bioinformatics data and our previous report (Fig. 5D, Fig. 8).

3.7 ZBH-01 induces G_0/G_1-phase arrest and increases apoptosis in colon cancer cell lines

The above results showed that the gene expression features of LS174T cells treated with ZBH-01 were significantly altered compared to CPT-11 and SN38 groups. Most DEmRNAs were mainly involved in DNA replication, cell cycle, and P53 signal pathway. Thus, we evaluated the effects of ZBH-01 on the cell cycle and apoptosis by two colon cancer cell lines (LS174T and SW1116). The results showed that ZBH-01 preferably arrested tumor cells in the G_0/G_1 phase, while CPT-11 and SN38 arrested cells in the S phase (Fig. 6). Regarding apoptosis, ZBH-01 induced more apoptosis and necrosis than CPT-11 and SN38 (Fig. 7).

Considering the 14 cell cycle-related genes screened out in Fig. 5, the interaction between MYBL2 and CCNA2/CDK2 plays a decisive role in the cell cycle transition from the G_1 to the S phase [24–30]. The Western blot demonstrated that MYBL2, CCNA2, and CDK2 were repressed in the ZBH-01 group compared to CPT-11 and SN38 (Fig. 5E). However, the more precise interaction between these genes and their relationship with ZBH-01 needs to be further studied.

The cells' ability to undergo apoptosis can be a major determinant of drug sensitivity [20]. Thus, to further analyze the effects of ZBH-01 on cell apoptosis, we detected the changes in mitochondrial membrane potential (MMP) in LS174T cells after drug treatment. The results showed that the MMP of the ZBH-01 group was significantly higher than CPT-11 and SN38 groups. We further verified the expression of some genes related to apoptosis using qRT-PCR, although they were not in the selected module of the PPI network. Some genes, including APAF1, ATR, BAX, BIRC3, CCND1, CCNE2, CDK4, CDK6, CDKN1A, MCL1, MDM2, and NEK2 showed consistent expression trends with the NGS result; while other genes, including ATM, BCL2L1, BID, BIRC5, CASP3, CASP9, CYCS, MDM4, RB1, TP53, TEP1, XAF1, and XIAP, displayed inconsistent expression trends (Fig. 8).

3.8 ZBH-01 alters the expression of some important genes in colon cancer cells

Furthermore, the levels of other proteins related to the cell cycle and apoptosis were further analyzed by Western blot. The results showed that after treatment with 50 nmol/L ZBH-01, the levels of cleaved-Cas3 and cleaved-PARP increased (Fig. 9A). However, CPT-11 and SN38 treatment did not exhibit comparable activity at the same concentration. P53 is the effector of DNA damage. CPT-11, SN38, and ZBH-01 induced increased levels of p53 protein compared to controls (Fig. 8B), consistent with a previous report [18]. The Bax gene encodes a protein that promotes apoptosis. ZBH-01 and SN38 presented similar

effects on Bax levels (Fig. 9B). Meanwhile, CPT-11 was less effective for Bax upregulation. Furthermore, ZBH-01, CPT-11, and SN38 presented almost similar effects on Bcl-xL downregulation. The levels of activated caspase 3 in the ZBH-01 group were significantly higher compared to CPT-11 and SN38 groups (Fig. 9C and D).

3.9 ZBH-01 represses tumor growth of colon cancer in vivo.

Xenografts models derived from LS174T cells were used to evaluate the antitumor effects of ZBH-01 and CPT-11 *in vivo.* Compared to controls, tumor growth was significantly suppressed in CPT-11- and ZBH-01-treated groups (Fig. 10A, C and D). The dosage of ZBH-01 seemed to cause a lighter significant loss of body weight than CPT-11 (Fig. 10B).

4. Discussion

Colorectal cancer is one of the most common malignant tumors worldwide. Irinotecan (CPT-11), a classic chemotherapeutic agent, plays an important role in its clinical treatment [31]. However, the serious side effects caused by CPT-11 limit its applications. In the last three decades, many studies have reported the synthesis of CPT-11 derivatives to enhance cytotoxicity or minimize adverse events [16, 32, 33]. Unfortunately, no new analogs have been approved so far. Recently, we synthesized a novel CPT-11 derivative, ZBH-01, that showed a higher inhibitory effect on the development of colon tumors, both *in vivo* and *in vitro*. In the present study, we explored its molecular mechanisms and demonstrated that ZBH-01 has superior anti-tumor characteristics compared to CPT-11.

DNA topoisomerases, which can be divided into two categories: TOP1 and TOP2, are a class of enzymes that exist in the nucleus. They can catalyze the break and combination of DNA strands, thereby controlling the topological state of DNA. In abnormally proliferating tumor cells, TOP1 and TOP2 are highly expressed. Therefore, topoisomerase inhibitors are an important class of anti-tumor drugs [34]. CPT-11 is a TOP1 inhibitor that disturbs the catalytic cycle of TOP1 by stabilizing the reversible covalent enzyme-DNA cleavable complex. By forming a drug-enzyme-DNA ternary complex during DNA synthesis, CPT-11 triggers the formation of irreversible single-stranded DNA break [35]. Here, a natural amino acid glycine group was used to replace the 4-piperidinopiperidine group to overcome the metabolism drawback of CPT-11. By conjugating the amino group of glycine to the 10-position of SN-38 via a carbamate bond, ZBH-01 was synthesized with the carboxyl group converted to sodium salt to improve water solubility. Surprisingly, ZBH-01 showed more potent antitumor activity *in vitro* and was rapidly converted to the active SN-38 in both non-enzymatic physiological buffer (pH 7.4) and plasma. The AChE inhibition activity of ZBH-01 was also very lower than CPT-11. Nevertheless, the solubility of ZBH-01 is higher than SN38, about 25.6 mg/mL (sodium salt of ZBH-01) in deionized water, facilitating its absorption. Moreover, the bioconversion of ZBH-01 to the active SN-38 is higher than CPT-11 both in non-enzymatic physiological buffer (pH 7.4) and plasma, which might also contribute to its antitumor potency.

Furthermore, we compared the inhibitory effects of ZBH-01 and CPT-11/SN38 on TOP1 in colon cancer cells. The DNA relaxation assay unexpectedly showed that the inhibition of ZBH-01 on TOP1 was significantly lower than CPT-11 and SN38. This was inconsistent with our previous reports [9, 11]. Then, we confirmed this result using NGS and qRT-PCR. However, the Western blot showed that TOP1 protein was slightly downregulated by ZBH-01, suggesting that ZBH-01 might inhibit TOP1 after transcription. Moreover, we observed that the levels of TOP2A mRNA were significantly repressed in the ZBH-01 group by NGS and qRT-PCR. Hence, we hypothesized that this might be related to the chemical structure of ZBH-01 but we did not explore this problem that requires more accurate experimental designs. We intend to explore these issues in the future.

High-throughput-based gene expression profiling enables the characterization of the relative drug sensitivity of cancer cells [36] and the identification of new drug targets [19]. Thus, to study the ZBH-01 mechanisms, we performed NGS to compare the mRNA expression profiles in colon cancer cells treated with ZBH-01, CPT-11, and SN38. The results showed that ZBH-01 treatment remarkably induced a unique abnormal expression of 1769 DEmRNAs (842 downregulated and 927 upregulated mRNAs) in LS174T cells. The GO and KEGG analysis showed that these DEmRNAs were mainly enriched in DNA replication, p53 signaling pathway, and cell cycle. Then, we filtered one prominent module of the PPI network, consisting of 73 genes mostly associated with the cell cycle. We found that TOP2A was in the center of the module, demonstrating its importance again.

From the above module, we verified the expression of the genes involved in the cell cycle by qRT-PCR. We also verified the expression of other key genes involved in apoptosis, such as BAX, BCL2L1, BID, BIRC3, and BIRC5. Except for a few genes, the expression trend was consistent between NGS and qRT-PCR. There are many reasons for this inconsistency, such as the inaccurate conduction of the experiment, design of primers, and low sample and experimental repetitions.

Then, we performed cell cycle and apoptosis analyses to explore the antitumor activity of ZBH-01. Under the same experimental conditions (50 nmol/L, 24 h), ZBH-01 significantly induced more apoptosis and cell cycle arrest in the G_1 phase in LS174T and SW1116 colon cancer cells; while CPT-11 and SN38 mainly induced cell cycle arrest in the S phase. However, they did not induce apoptosis even 48 and 72 h after treatment. At 12 and 18 h, the results showed a similar trend, with ZBH-01 presenting a stronger effect on inducing tumor cell apoptosis. These results were further verified by the MMP and Western blot assays and were consistent with other reports [18].

The members of the BCL2 family are implicated in the intrinsic apoptotic pathway. These proteins can be either pro-apoptotic (BAX and BBC3) or anti-apoptotic (BCL2, BCL2L1, and MCL1) [37]. In our present study, the levels of BAX protein significantly increased, while Bcl-xL decreased after ZBH-01 exposure. Accordingly, the levels of active caspase 3 and cleaved-PARP increased after ZBH-01 treatment. The tumor suppressor P53 is a key regulator in various signaling pathways including DNA damage, cell cycle, and apoptosis [38]. Here, p53 was upregulated after CPT-11, SN38, and ZBH-01 treatments. Among them, ZBH-01 had the strongest effect. These results were consistent with other studies that reported increased

expression of p53 after CPT treatment leading to cell cycle arrest [39], and CPT-11 inducing cell cycle arrest in the S- and G_2/M-phases [40].

Previous studies have shown that the transcription factor MYBL2 can activate CDC2 and cyclin D1 after being phosphorylated by cyclin A/CDK2. The interaction between these genes plays a decisive role in regulating the transition from the G_1 to the S phase. All these genes were detected in our filtered module. Therefore, we verified their levels by qRT-PCR and Western blot. The results showed that the protein levels of CCNA2, CDK2, and MYBL2 were more repressed by ZBH-01 in colon cancer cells compared to treatment with CPT-11 and SN38. This might preliminarily explain our cell cycle experimental results in which ZBH-01 induced cell cycle arrest in the G_1 phase (Fig. 11).

Finally, ZBH-01 presented antitumor activity *in vivo* and comparable tumor inhibitory potential and lower toxicity to CPT-11. These results demonstrated that ZBH-01 is worthy of further studies.

Our study also has some limitations. First, we should analyze more tumor cell lines and other tumor models in mice. Second, we only verified the levels of some DEmRNAs by qRT-PCR. Neither the expressions of gene-encoded proteins nor the gain of or loss of function was evaluated. Furthermore, we did not add corresponding agonists or antagonists to help analyze the mechanisms of ZBH-01. Additionally, there are actual differences between the expression patterns of DEmRNAs in colon cancer tissues and cell lines after drug treatments, and how to fully elucidate these differences might be considered in the future.

In summary, we demonstrated that ZBH-01, a new CPT-11 analog, has a broad spectrum of antiproliferative activity in various human tumor cell lines. By inducing cell cycle arrest and promoting apoptosis, ZBH-01 presented superior antitumor efficacy compared to both CPT-11 and SN38. Finally, ZBH-01 also showed higher tolerability than CPT-11 *in vivo*.

Abbreviation

BUB1	BUB1 mitotic checkpoint serine/threonine kinase
BUB1B	BUB1 mitotic checkpoint serine/threonine kinase B
CCNA2	cyclin A2
CDC20	cell division cycle 20
CDC25C	cell division cycle 25C
CDC45	cell division cycle 45
CDC7	cell division cycle 7
CDK2	cyclin dependent kinase 2
CHEK1 (CHK1)	checkpoint kinase 1
E2F8	E2F transcription factor 8
EZH2	enhancer of zeste 2 polycomb repressive complex 2 subunit
FOXM1	forkhead box M1
MCM3	minichromosome maintenance complex component 3
MCM7	minichromosome maintenance complex component 7
MYBL2	MYB proto-oncogene like 2
ORC1	origin recognition complex subunit 1
PKMYT1	protein kinase, membrane associated tyrosine/threonine 1
RAD54L	RAD54 like
TOP1	DNA topoisomerase I
TOP2A	DNA topoisomerase II alpha
TTK	TTK protein kinase
APAF1	apoptotic peptidase activating factor 1
ATM	Ataxia telangiectasia mutated
ATR	Ataxia telangiectasia related
BAX	BCL2 associated X, apoptosis regulator
BCL2L1	BCL2 like 1
BID	BH3 interacting domain death agonist
BIRC3 (c-IAP2)	baculoviral IAP repeat containing 3
BIRC5 (survivin)	baculoviral IAP repeat containing 5

CASP3	caspase 3
CASP9	caspase 9
CCND1	cyclin D1
CCNE2	cyclin E2
CDK4	cyclin dependent kinase 4
CDK6	cyclin dependent kinase 6
CDKN1A (P21)	cyclin dependent kinase inhibitor 1A
CYCS	cytochrome c, somatic
MCL1	MCL1 apoptosis regulator, BCL2 family member
MDM2	MDM2 proto-oncogene
MDM4	MDM4 regulator of p53
NEK2	NIMA related kinase 2
RB1	RB transcriptional corepressor 1
TP53	tumor protein p53
TEP1	telomerase associated protein 1
XAF1	XIAP associated factor 1
XIAP (BIRC4)	X-linked inhibitor of apoptosis
PARP	poly-ADP-ribose-polymerase

Declarations

Author Contributions

YL designed and performed most of the experiments; HY conceived of the study and wrote the manuscript; MY and ZW conducted qRT-PCR; DZ and WZ contributed to the DNA relaxation assay; SL and ZG assist in *in vivo* experiments; ZT provided reagents; WS synthesized and provided ZBH-01. DW and HY supervised all aspects of the study. All authors read and approved the final manuscript.

Funding

The present study was supported by funding of the Natural Science Foundation of Jilin Province (to D.W., grant no. 20200201479JC).

Availability of data and materials

All data and materials related in this research are available for sharing.

Ethics approval and consent to participate

The study was approved by the Institutional Review Board (IRB) of The First Hospital of Jilin University. All subjects were provided a written informed consent.

Consent for publication

I give my consent for the article to publish in Journal of translational medicine, section of tumor chemotherapy.

Competing interests

The authors declare that they have no conflict of interest.

Acknowledgements

We thank Prof Hubing Shi and Dr. Jing Yu from Sichuan University for assistance with bioinformatic analysis.

References

1. R.M. Feng, Y.N. Zong, S.M. Cao, R.H. Xu, Current cancer situation in China: good or bad news from the 2018 Global Cancer Statistics?, Cancer Commun (Lond) 39(1) (2019) 22.
2. W. Chen, R. Zheng, P.D. Baade, S. Zhang, H. Zeng, F. Bray, A. Jemal, X.Q. Yu, J. He, Cancer statistics in China, 2015, CA Cancer J Clin 66(2) (2016) 115-32.
3. K.-i. Fujita, Y. Kubota, H. Ishida, Y. Sasaki, Irinotecan, a key chemotherapeutic drug for metastatic colorectal cancer, World journal of gastroenterology 21(43) (2015) 12234-12248.
4. A. Thomas, Y. Pommier, Targeting Topoisomerase I in the Era of Precision Medicine, Clin Cancer Res 25(22) (2019) 6581-6589.
5. Y. Pommier, Drugging topoisomerases: lessons and challenges, ACS chemical biology 8(1) (2013) 82-95.
6. F. Li, T. Jiang, Q. Li, X. Ling, Camptothecin (CPT) and its derivatives are known to target topoisomerase I (Top1) as their mechanism of action: did we miss something in CPT analogue molecular targets for treating human disease such as cancer?, American journal of cancer research 7(12) (2017) 2350-2394.
7. J.-M. Yuan, N.-Y. Chen, H.-R. Liao, G.-H. Zhang, X.-J. Li, Z.-Y. Gu, C.-X. Pan, D.-L. Mo, G.-F. Su, 3-(Benzo[d]thiazol-2-yl)-4-aminoquinoline derivatives as novel scaffold topoisomerase I inhibitor via DNA intercalation: design, synthesis, and antitumor activities, New Journal of Chemistry 44(26) (2020) 11203-11214.

8. E. Foto, Ç. Özen, F. Zilifdar, B. Tekiner-Gülbaş, İ. Yıldız, E. Akı-Yalçın, N. Diril, İ. Yalçın, Benzoxazines as new human topoisomerase I inhibitors and potential poisons, DARU Journal of Pharmaceutical Sciences 28(1) (2020) 65-73.
9. D. Wu, W. Shi, J. Zhao, Z. Wei, Z. Chen, D. Zhao, S. Lan, J. Tai, B. Zhong, H. Yu, Assessment of the chemotherapeutic potential of a new camptothecin derivative, ZBH-1205, Arch Biochem Biophys 604 (2016) 74-85.
10. M. Zhou, M. Liu, X. He, H. Yu, D. Wu, Y. Yao, S. Fan, P. Zhang, W. Shi, B. Zhong, Synthesis and biological evaluation of novel 10-substituted-7-ethyl-10-hydroxycamptothecin (SN-38) prodrugs, Molecules 19(12) (2014) 19718-31.
11. D. Wu, D.W. Zhao, Y.Q. Li, W.G. Shi, Q.L. Yin, Z.K. Tu, Y.Y. Yu, B.H. Zhong, H. Yu, W.G. Bao, Antitumor potential of a novel camptothecin derivative, ZBH-ZM-06, Oncol Rep 39(2) (2018) 871-879.
12. K.J. Livak, T.D. Schmittgen, Analysis of relative gene expression data using real-time quantitative PCR and the 2(-Delta Delta C(T)) Method, Methods 25(4) (2001) 402-8.
13. G. Yu, L.-G. Wang, Y. Han, Q.-Y. He, clusterProfiler: an R package for comparing biological themes among gene clusters, Omics : a journal of integrative biology 16(5) (2012) 284-287.
14. D. Szklarczyk, A. Franceschini, S. Wyder, K. Forslund, D. Heller, J. Huerta-Cepas, M. Simonovic, A. Roth, A. Santos, K.P. Tsafou, M. Kuhn, P. Bork, L.J. Jensen, C. von Mering, STRING v10: protein-protein interaction networks, integrated over the tree of life, Nucleic acids research 43(Database issue) (2015) D447-D452.
15. P. Shannon, A. Markiel, O. Ozier, N.S. Baliga, J.T. Wang, D. Ramage, N. Amin, B. Schwikowski, T. Ideker, Cytoscape: a software environment for integrated models of biomolecular interaction networks, Genome research 13(11) (2003) 2498-2504.
16. D.-Z. Li, Q.-Z. Zhang, C.-Y. Wang, Y.-L. Zhang, X.-Y. Li, J.-T. Huang, H.-Y. Liu, Z.-D. Fu, H.-X. Song, J.-P. Lin, T.-F. Ji, X.-D. Pan, Synthesis and antitumor activity of novel substituted uracil-1'(N)-acetic acid ester derivatives of 20(S)-camptothecins, European Journal of Medicinal Chemistry 125 (2017) 1235-1246.
17. R. Cincinelli, L. Musso, R. Artali, M.B. Guglielmi, I. La Porta, C. Melito, F. Colelli, F. Cardile, G. Signorino, A. Fucci, M. Frusciante, C. Pisano, S. Dallavalle, Hybrid topoisomerase I and HDAC inhibitors as dual action anticancer agents, PloS one 13(10) (2018) e0205018-e0205018.
18. J. Zou, S. Li, Z. Chen, Z. Lu, J. Gao, J. Zou, X. Lin, Y. Li, C. Zhang, L. Shen, A novel oral camptothecin analog, gimatecan, exhibits superior antitumor efficacy than irinotecan toward esophageal squamous cell carcinoma in vitro and in vivo, Cell Death Dis 9(6) (2018) 661.
19. J. Barretina, G. Caponigro, N. Stransky, K. Venkatesan, A.A. Margolin, S. Kim, C.J. Wilson, J. Lehár, G.V. Kryukov, D. Sonkin, A. Reddy, M. Liu, L. Murray, M.F. Berger, J.E. Monahan, P. Morais, J. Meltzer, A. Korejwa, J. Jané-Valbuena, F.A. Mapa, J. Thibault, E. Bric-Furlong, P. Raman, A. Shipway, I.H. Engels, J. Cheng, G.K. Yu, J. Yu, P. Aspesi, Jr., M. de Silva, K. Jagtap, M.D. Jones, L. Wang, C. Hatton, E. Palescandolo, S. Gupta, S. Mahan, C. Sougnez, R.C. Onofrio, T. Liefeld, L. MacConaill, W. Winckler, M. Reich, N. Li, J.P. Mesirov, S.B. Gabriel, G. Getz, K. Ardlie, V. Chan, V.E. Myer, B.L. Weber, J. Porter, M.

Warmuth, P. Finan, J.L. Harris, M. Meyerson, T.R. Golub, M.P. Morrissey, W.R. Sellers, R. Schlegel, L.A. Garraway, The Cancer Cell Line Encyclopedia enables predictive modelling of anticancer drug sensitivity, Nature 483(7391) (2012) 603-607.

20. J.M. Mariadason, D. Arango, Q. Shi, A.J. Wilson, G.A. Corner, C. Nicholas, M.J. Aranes, M. Lesser, E.L. Schwartz, L.H. Augenlicht, Gene expression profiling-based prediction of response of colon carcinoma cells to 5-fluorouracil and camptothecin, Cancer Res 63(24) (2003) 8791-812.
21. S. Lalevée, R. Feil, Long noncoding RNAs in human disease: emerging mechanisms and therapeutic strategies, Epigenomics 7(6) (2015) 877-879.
22. D. Szklarczyk, J.H. Morris, H. Cook, M. Kuhn, S. Wyder, M. Simonovic, A. Santos, N.T. Doncheva, A. Roth, P. Bork, L.J. Jensen, C. von Mering, The STRING database in 2017: quality-controlled protein-protein association networks, made broadly accessible, 45(D1) (2017) D362-D368.
23. G.D. Bader, C.W. Hogue, An automated method for finding molecular complexes in large protein interaction networks, BMC bioinformatics 4 (2003) 2.
24. C. Müller-Tidow, W. Wang, G.E. Idos, S. Diederichs, R. Yang, C. Readhead, W.E. Berdel, H. Serve, M. Saville, R. Watson, H.P. Koeffler, Cyclin A1 directly interacts with B-myb and cyclin A1/cdk2 phosphorylate B-myb at functionally important serine and threonine residues: tissue-specific regulation of B-myb function, Blood 97(7) (2001) 2091-2097.
25. V. Tripathi, Z. Shen, A. Chakraborty, S. Giri, S.M. Freier, X. Wu, Y. Zhang, M. Gorospe, S.G. Prasanth, A. Lal, K.V. Prasanth, Long noncoding RNA MALAT1 controls cell cycle progression by regulating the expression of oncogenic transcription factor B-MYB, PLoS Genet 9(3) (2013) e1003368-e1003368.
26. O. Bartsch, S. Horstmann, K. Toprak, K.-H. Klempnauer, S. Ferrari, Identification of cyclin A/Cdk2 phosphorylation sites in B-Myb, European Journal of Biochemistry 260(2) (1999) 384-391.
27. Y. Tian, H. Chen, L. Qiao, W. Zhang, J. Zheng, W. Zhao, J.J. Chen, W. Zhang, CIP2A facilitates the G1/S cell cycle transition via B-Myb in human papillomavirus 16 oncoprotein E6-expressing cells, Journal of cellular and molecular medicine 22(9) (2018) 4150-4160.
28. M. Bessa, M.K. Saville, R.J. Watson, Inhibition of cyclin A/Cdk2 phosphorylation impairs B-Myb transactivation function without affecting interactions with DNA or the CBP coactivator, Oncogene 20(26) (2001) 3376-3386.
29. C. Petrovas, S. Jeay, R.E. Lewis, G.E. Sonenshein, B-Myb repressor function is regulated by cyclin A phosphorylation and sequences within the C-terminal domain, Oncogene 22(13) (2003) 2011-2020.
30. Z. Guan, W. Cheng, D. Huang, A. Wei, High MYBL2 expression and transcription regulatory activity is associated with poor overall survival in patients with hepatocellular carcinoma, Current Research in Translational Medicine 66(1) (2018) 27-32.
31. T. Takaoka, T. Kimura, R. Shimoyama, S. Kawamoto, K. Sakamoto, F. Goda, H. Miyamoto, Y. Negoro, A. Tsuji, K. Yoshizaki, T. Goji, S. Kitamura, H. Yano, K. Okamoto, M. Kimura, T. Okahisa, N. Muguruma, Y. Niitsu, T. Takayama, Panitumumab in combination with irinotecan plus S-1 (IRIS) as second-line therapy for metastatic colorectal cancer, Cancer Chemotherapy and Pharmacology 78(2) (2016) 397-403.

32. X.Y. Yang, H.Y. Zhao, H. Lei, B. Yuan, S. Mao, M. Xin, S.Q. Zhang, Synthesis and Biological Evaluation of 10-Substituted Camptothecin Derivatives with Improved Water Solubility and Activity, ChemMedChem 16(6) (2020) 1000-1010.
33. Z. Chen, Z. Liu, W. Huang, Z. Li, J. Zou, J. Wang, X. Lin, B. Li, D. Chen, Y. Hu, J. Ji, J. Gao, L. Shen, Gimatecan exerts potent antitumor activity against gastric cancer in vitro and in vivo via AKT and MAPK signaling pathways, J Transl Med 15(1) (2017) 253-253.
34. Y. Pommier, Y. Sun, S.N. Huang, J.L. Nitiss, Roles of eukaryotic topoisomerases in transcription, replication and genomic stability, Nature reviews. Molecular cell biology 17(11) (2016) 703-721.
35. C. Bailly, Irinotecan: 25 years of cancer treatment, Pharmacological Research 148 (2019) 104398.
36. M.M. Arroyo, A. Berral-González, S. Bueno-Fortes, D. Alonso-López, J.D.L. Rivas, Mining Drug-Target Associations in Cancer: Analysis of Gene Expression and Drug Activity Correlations, Biomolecules 10(5) (2020) 667.
37. P.E. Czabotar, G. Lessene, A. Strasser, J.M. Adams, Control of apoptosis by the BCL-2 protein family: implications for physiology and therapy, Nature Reviews Molecular Cell Biology 15(1) (2014) 49-63.
38. J. Chen, The Cell-Cycle Arrest and Apoptotic Functions of p53 in Tumor Initiation and Progression, Cold Spring Harbor perspectives in medicine 6(3) (2016) a026104-a026104.
39. W.A. Cliby, K.A. Lewis, K.K. Lilly, S.H. Kaufmann, S Phase and G2 Arrests Induced by Topoisomerase I Poisons Are Dependent on ATR Kinase Function, Journal of Biological Chemistry 277(2) (2002) 1599-1606.
40. D.K. Maurya, R. Ayuzawa, C. Doi, D. Troyer, M. Tamura, Topoisomerase I inhibitor SN-38 effectively attenuates growth of human non-small cell lung cancer cell lines in vitro and in vivo, Journal of environmental pathology, toxicology and oncology : official organ of the International Society for Environmental Toxicology and Cancer 30(1) (2011) 1-10.

Figures

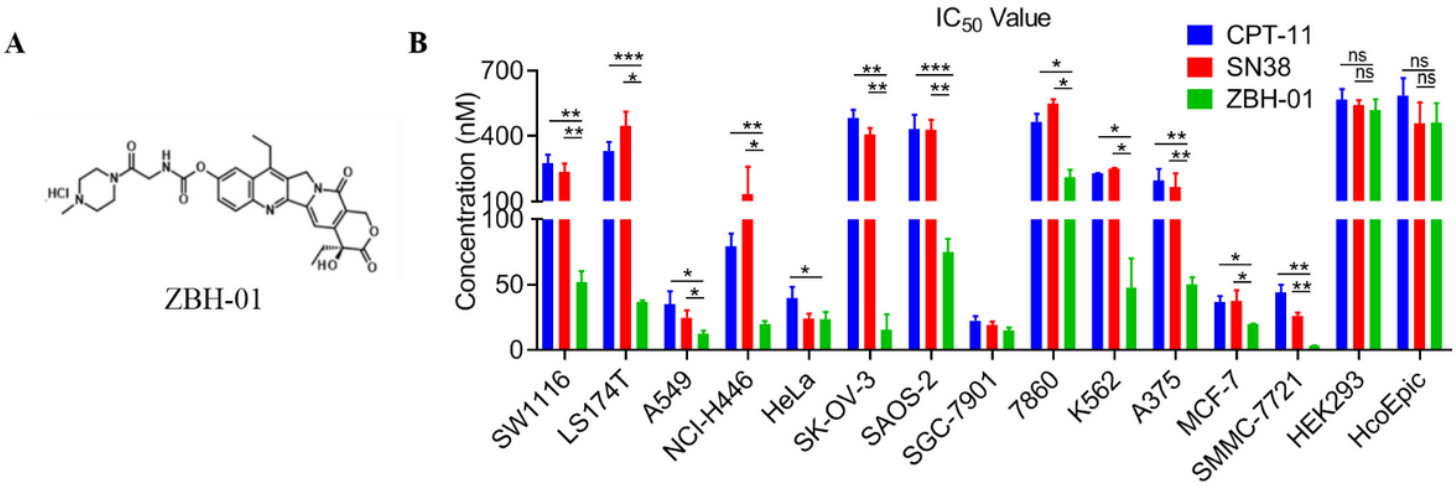

Figure 1

Comparison of IC_{50} values (nmol/L) between drug treatment groups. (A) Chemical structure of ZBH-01. (B) Detection of cell proliferation activity by MTT or CCK8 after drug treatments. SW1116 and LS174T, colon adenocarcinoma. A549 and NCI-H446, non-small cell lung cancer. HeLa, cervical carcinoma. SK-OV-3, ovarian cancer. SAOS-2, osteosarcoma. SGC-7901, gastric adenocarcinoma. 7860, renal carcinoma. K562, chronic myelogenous leukemia. A375, melanoma. MCF-7, breast cancer. SMMC-7721, hepatoma. HcoEpic, human colon mucosal epithelia. HEK293, human embryonic kidney cell. ANOVA & two-tailed t-test, n = 3. *$p < 0.05$,**$p < 0.01$, ***$p < 0.001$.

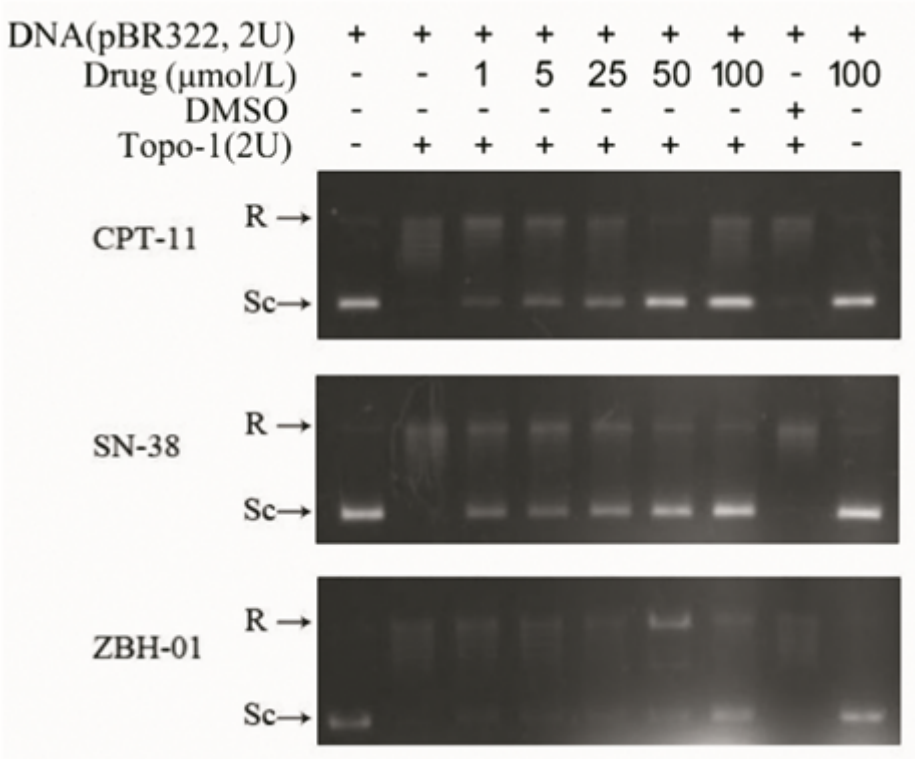

Figure 2

Inhibitory effect of ZBH-01 on TOP1. TOP1-catalyzed DNA relaxation was inhibited by CPT-11, SN-38, and ZBH-01. The DNA strand breakage induced by TOP1 was evaluated by the conversion of the double-stranded supercoiled DNA to a relaxed form. The position of supercoiled DNA (Sc) and relaxed DNA (R) are indicated.

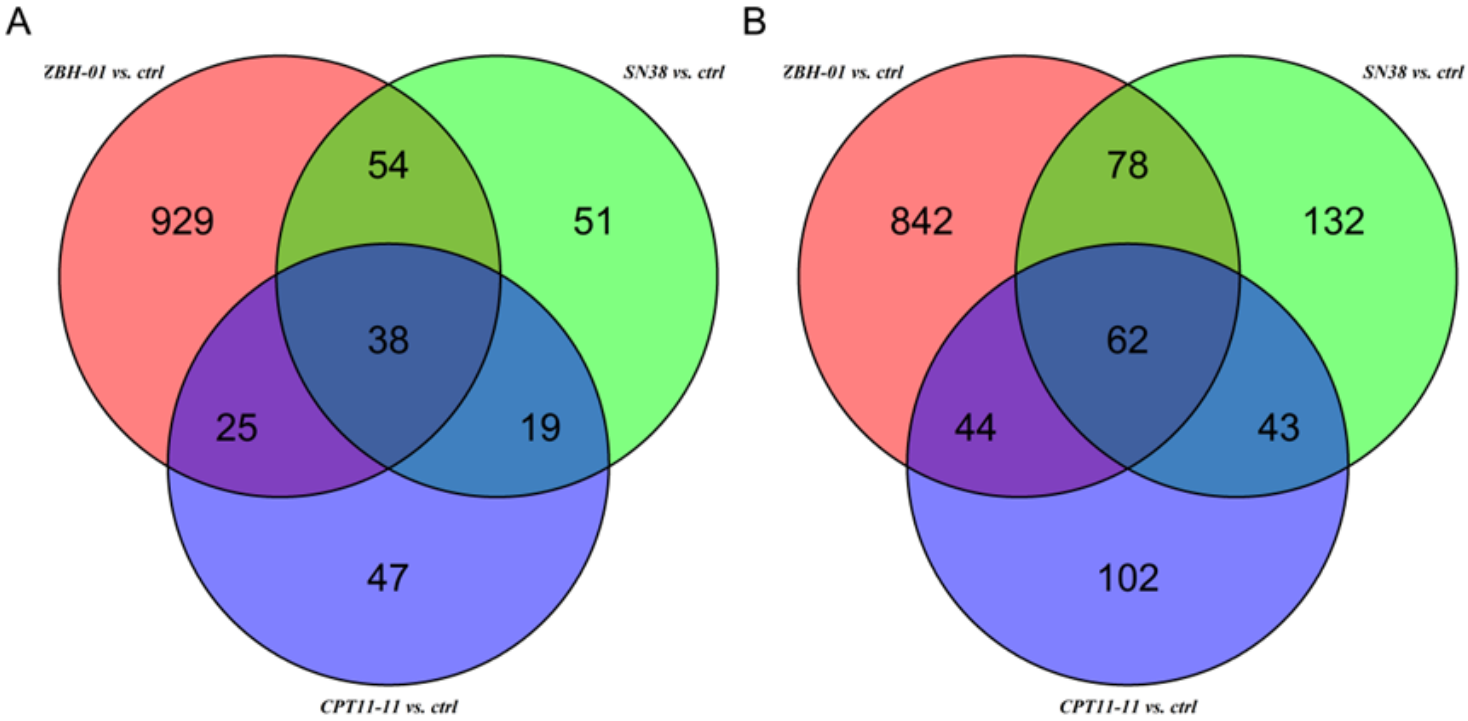

Figure 3

Venn diagrams for differentially expressed genes among ZBH-01, CPT-11, and SN38 groups. A: Upregulated genes; B: Downregulated genes.

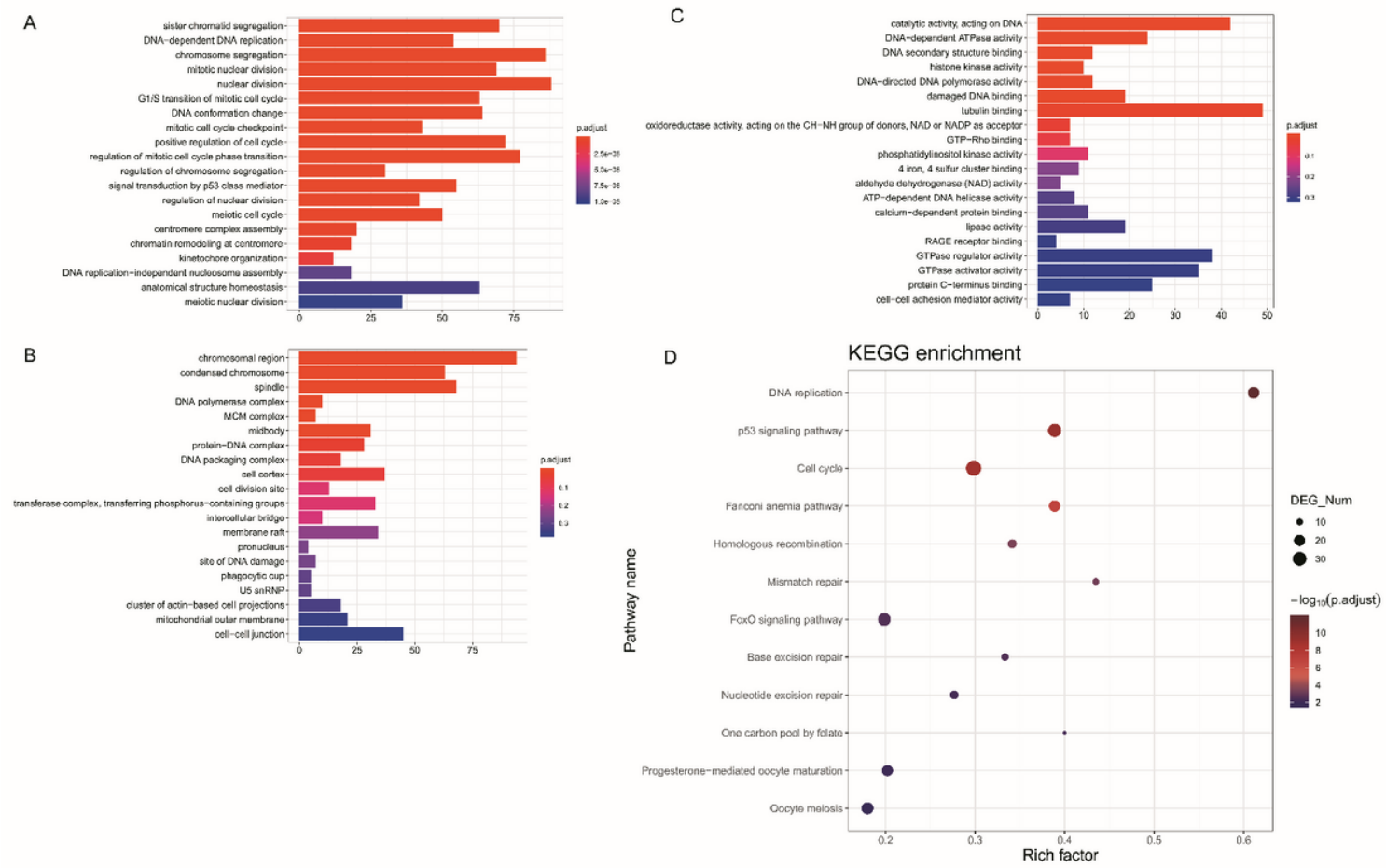

Figure 4

Significantly enriched GO terms and KEGG pathways for the DEmRNAs in the ZBH-01-treated group. A: biological processes (BP). B: cellular components (CC). C: molecular functions (MF). D: KEGG pathways.

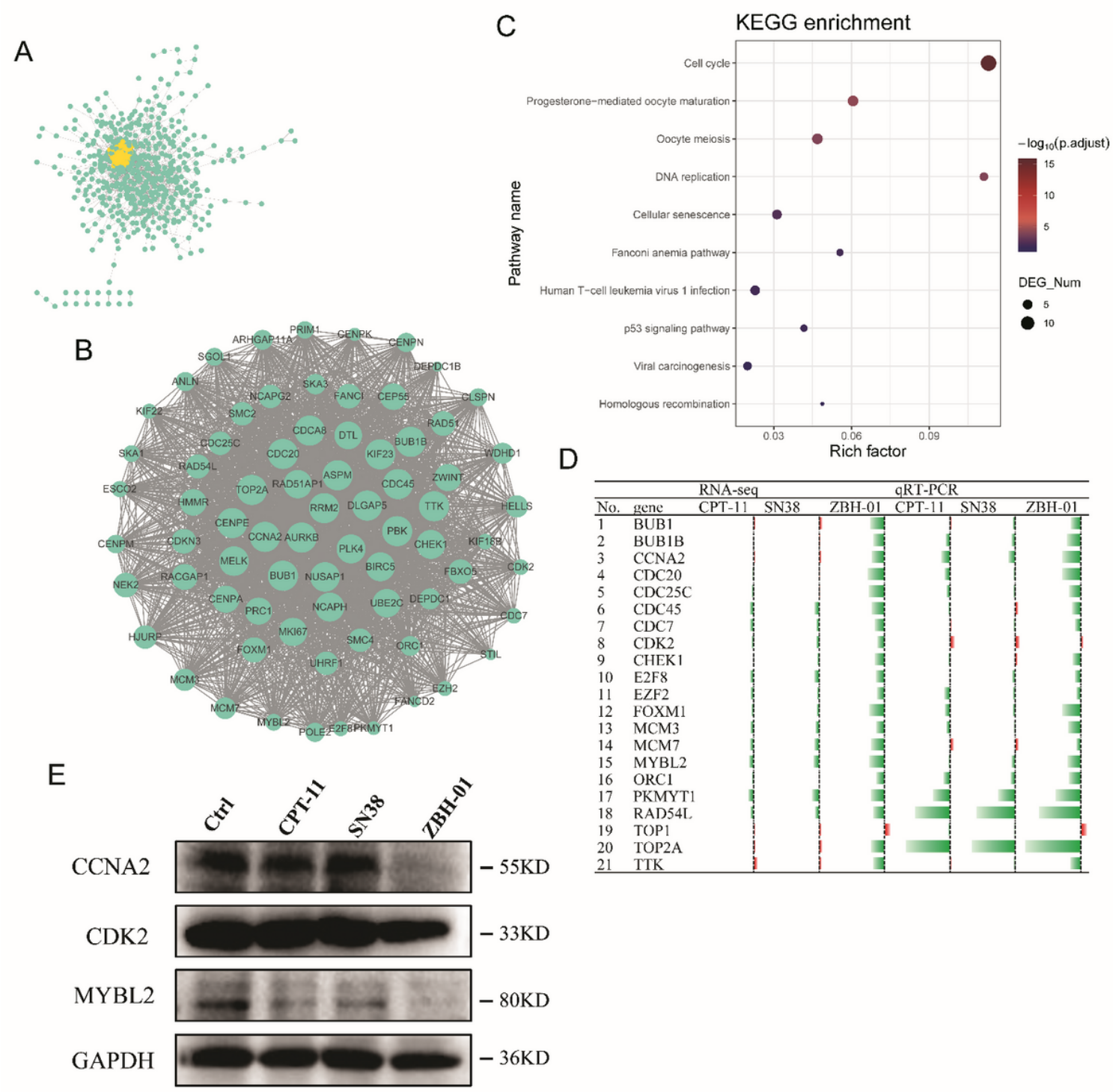

Figure 5

The proteins encoded by ZBH-01 group-specific DEmRNAs were prominently involved in cell cycle regulation A: The PPI network. The yellow part highlights the most prominent module. B: Enlargement of the yellow module in (A), containing 73 genes. C: Most significantly enriched KEGG pathway of these 73 genes. D: Relative expression of some DEmRNAs in (B) in LS174T cells after treatment with 50 nmol/L ZBH-01, CPT-11, and SN38 24 h (logarithmic transformation). Green: downregulated; Red: upregulated. E: Western blot of three representative genes related to cell cycle regulation.

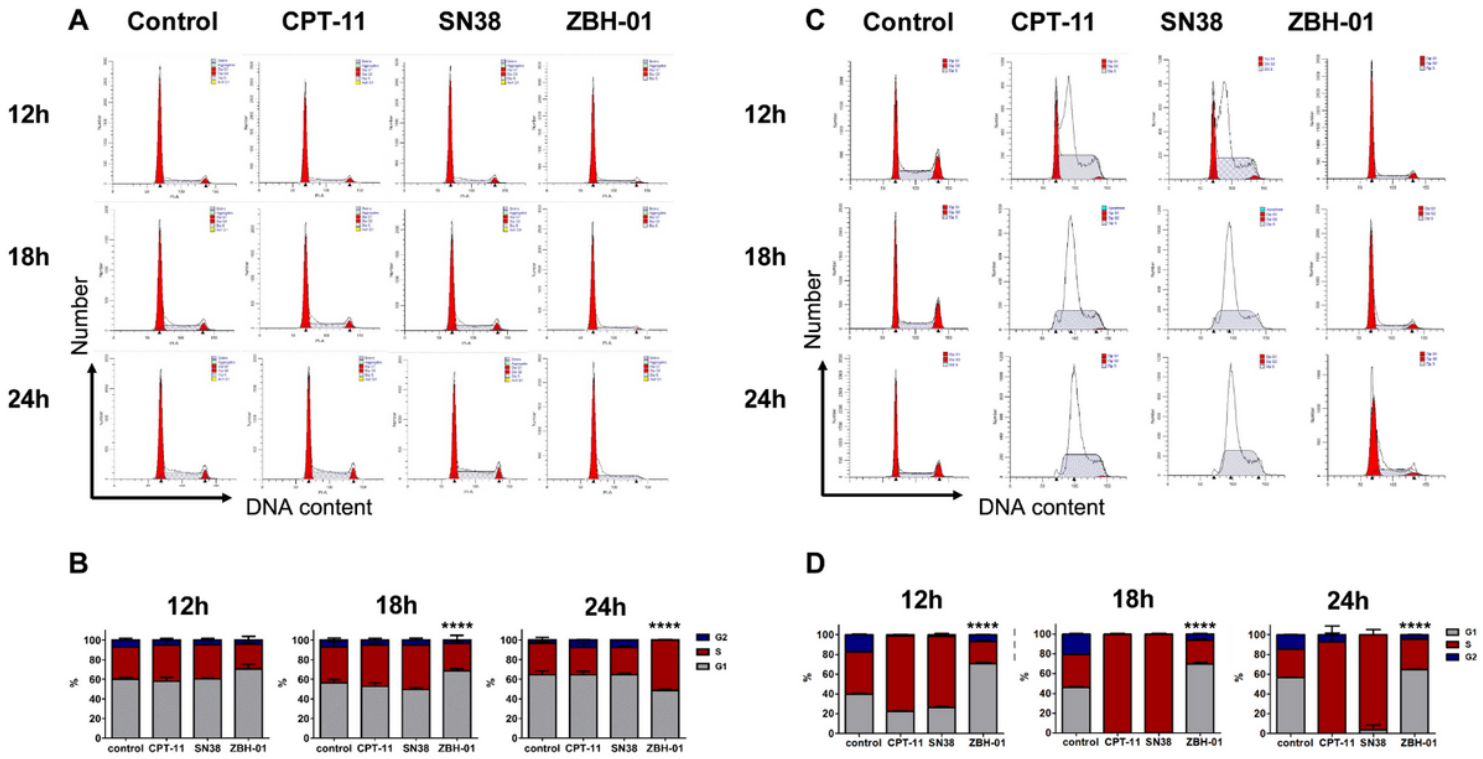

Figure 6

Cell cycle alteration in response to drug treatments. LS174T and SW1116 cells were treated with 50 nmol/L ZBH-01, CPT-11, and SN38 for 12, 18, and 24 h. The percentage of cells in G_0/G_1, S, and G_2/M phases were analyzed by flow cytometry. A: Histograms of cell cycle distribution of LS174T cells at different time points. B: Statistical analysis of A. 12 h: $\chi^2 = 7.5391$, $p = 0.2738$; 18 h: $\chi^2 = 40.6417$, $^{****}p < 0.0001$; 24 h: $\chi^2 = 60.8731$, $^{****}p < 0.0001$ C: Histograms of cell cycle distribution of SW1116 cells at different times. D: Statistical analysis of C. 12 h: $\chi^2 = 96.9852$, $^{****}p < 0.0001$; 18 h: $\chi^2 = 242.4146$, $^{****}p < 0.0001$; 24 h: $\chi^2 = 197.4546$, $^{****}p < 0.0001$. ANOVA & two-tailed t-test, n = 3.

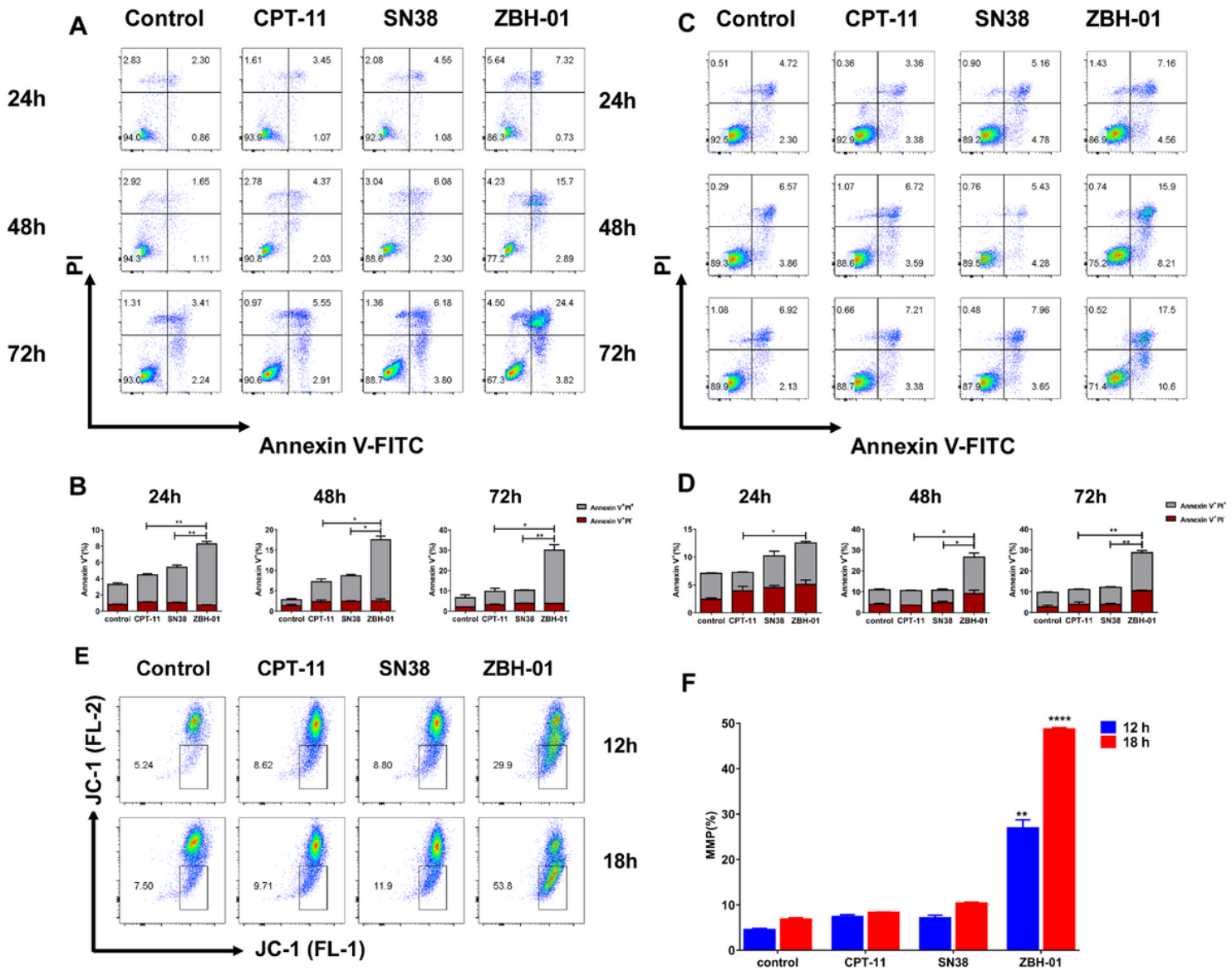

Figure 7

Induction of tumor cell apoptosis by ZBH-01, CPT-11, and SN38 (50 nmol/L, 24 h). A: Scatter diagrams of apoptosis of SW1116 cells at different times. B: Statistical analysis of A. Annexin V^+/PI^- (%), 12 h: $^*p$ = 0.0176, ZBH-01 vs. CPT-11. 48 h: $^*p$ = 0.0284, ZBH-01 vs. CPT-11. 72 h: $^{**}p$ = 0.0047, ZBH-01 vs. CPT-11; $^{**}p$ = 0.0067, ZBH-01 vs. SN38. ANOVA & two-tailed t-test, n = 3. C: Scatter diagrams of apoptosis of LS174T cells at different times. D: Statistical analysis of C. Annexin V^+/PI^- (%), 12 h: $^*p$ = 0.0148, ZBH-01 vs. CPT-11; $^*p$ = 0.0124, ZBH-01 vs. SN38. 18 h: $^*p$ = 0.0341, ZBH-01 vs. CPT-11; $^*p$ = 0.0374, ZBH-01 vs. SN38. 24 h: $^*p$ = 0.0404, ZBH-01 vs. CPT-11; $^*p$ = 0.0299, ZBH-01 vs. SN38. 48 h: $^*p$ = 0.0399, ZBH-01 vs. SN38. 72 h: $^*p$ = 0.0073, ZBH-01 vs. CPT-11; $^{**}p$ = 0.0070, ZBH-01 vs. SN38. ANOVA & two-tailed t-test, n = 3. E: Scatter diagrams of MMP of LS174T cells in response to drug treatment (50 nmol/L) at different time points. F: Statistical analysis of E. 12 h: $^*p$ = 0.0178, ZBH-01 vs. SN38. 18 h: $^{**}p$ = 0.0047, ZBH-01 vs. CPT-11; $^{**}p$ = 0.0047, ZBH-01 vs. SN38. 24 h: $^{****}p < 0.0001$, ZBH-01 vs. CPT-11; $^{****}p < 0.0001$, ZBH-01 vs. SN38. ANOVA & two-tailed t-test, n = 2.

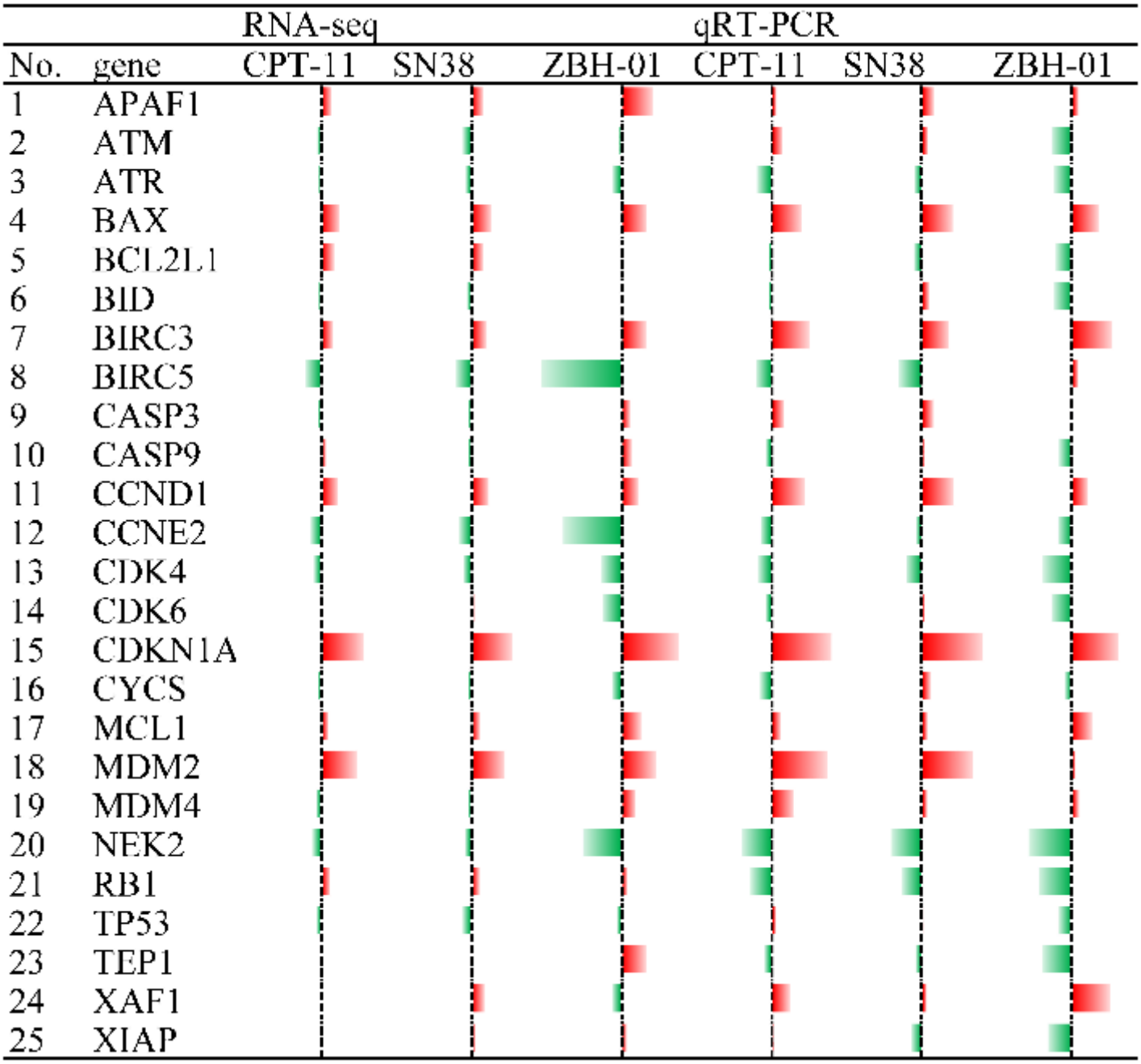

Figure 8

Relative mRNA expression of some differentially expressed genes involved in apoptosis in LS174T cells after treatment with 50 nmol/L ZBH-01, CPT-11, and SN38 24 h (logarithmic transformation). Green: downregulated; Red: upregulated.

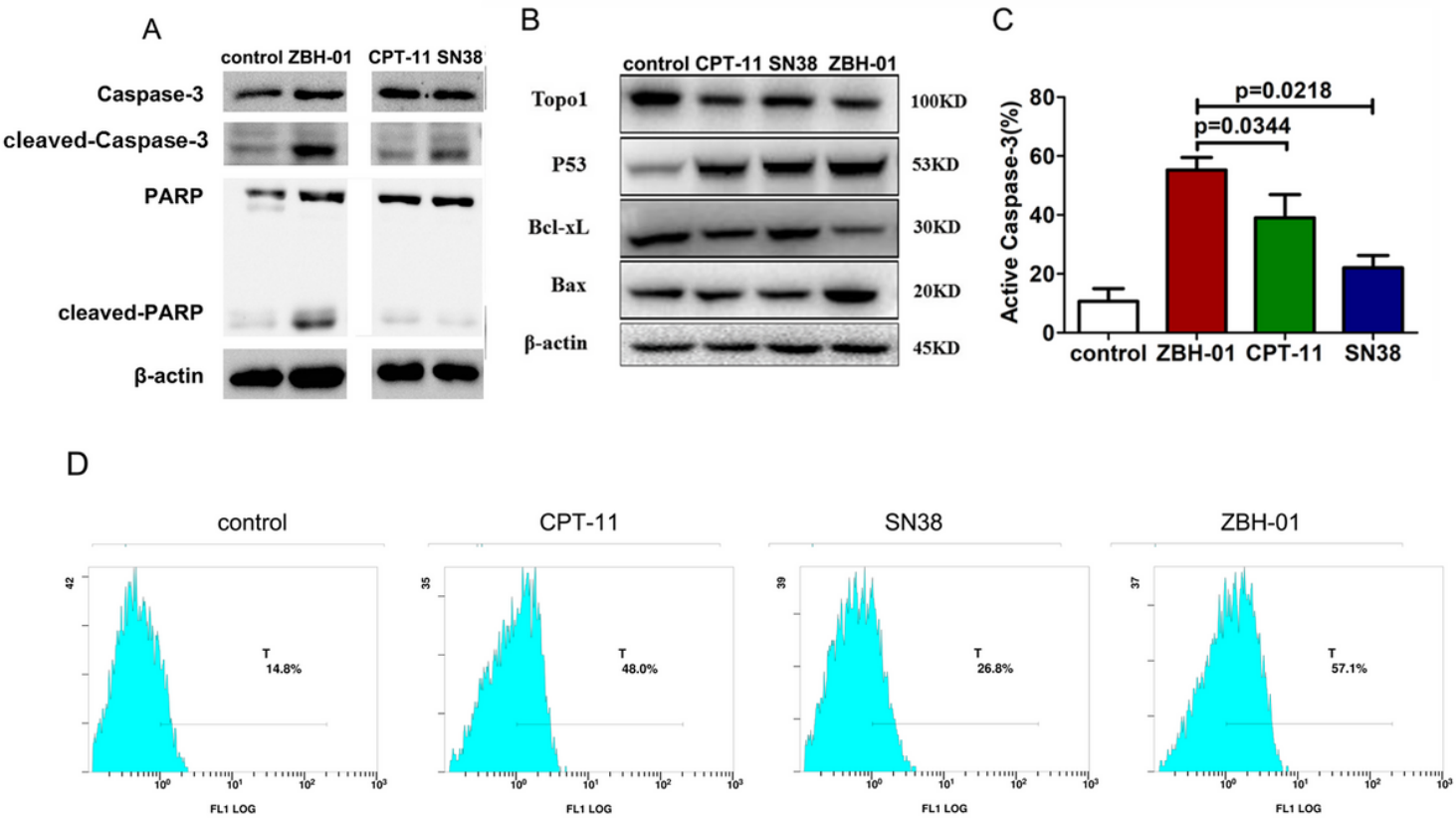

Figure 9

Levels of some important proteins in LS174T cells were determined after ZBH-01, CPT-11, and SN38 treatment (50 nmol/L) for 24 h, respectively. A and B: Western blots. C: Histogram of active caspase-3 levels. ANOVA & two-tailed t-test, n = 3. D: Representative graph of active caspase 3 percentage by flow cytometry.

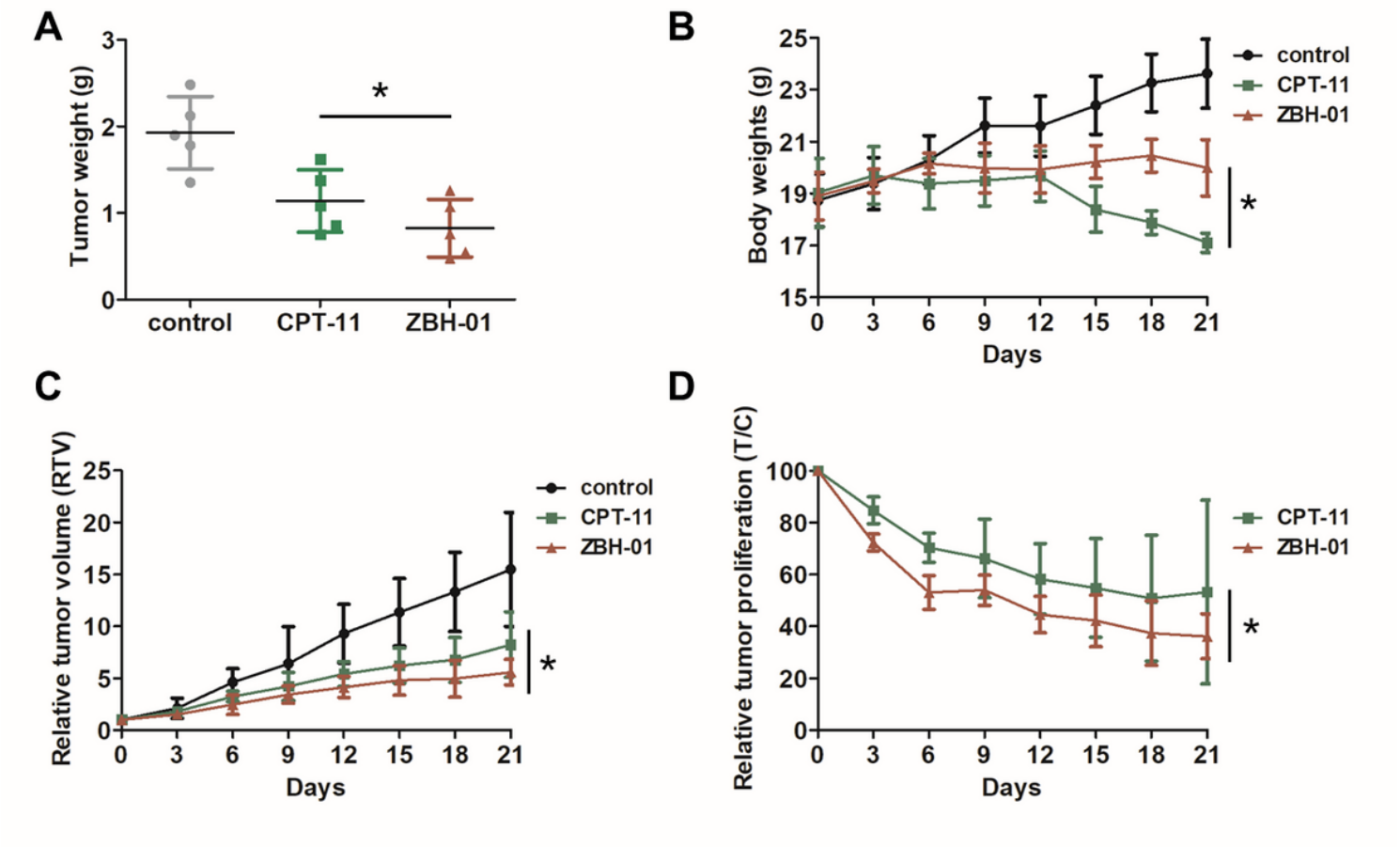

Figure 10

*A*ntitumor activity *in vivo* of ZBH-01 and CPT-11 in a nude mice colon cancer xenograft model. (A) Tumor weights (g) at the end of the experiment. $^{*}p$ = 0.01918, ZBH-01 vs. CPT-11. (B) Body weights (g) at various times. $^{*}p$ = 0.01412, ZBH-01 vs. CPT-11. (C) Relative tumor volumes at various times. $^{*}p$ = 0.03101, ZBH-01 vs. CPT-11. (D) Relative tumor proliferation at various times. $^{*}p$ = 0.02277, ZBH-01 vs. CPT-11. ANOVA & two-tailed t-test, n = 6.

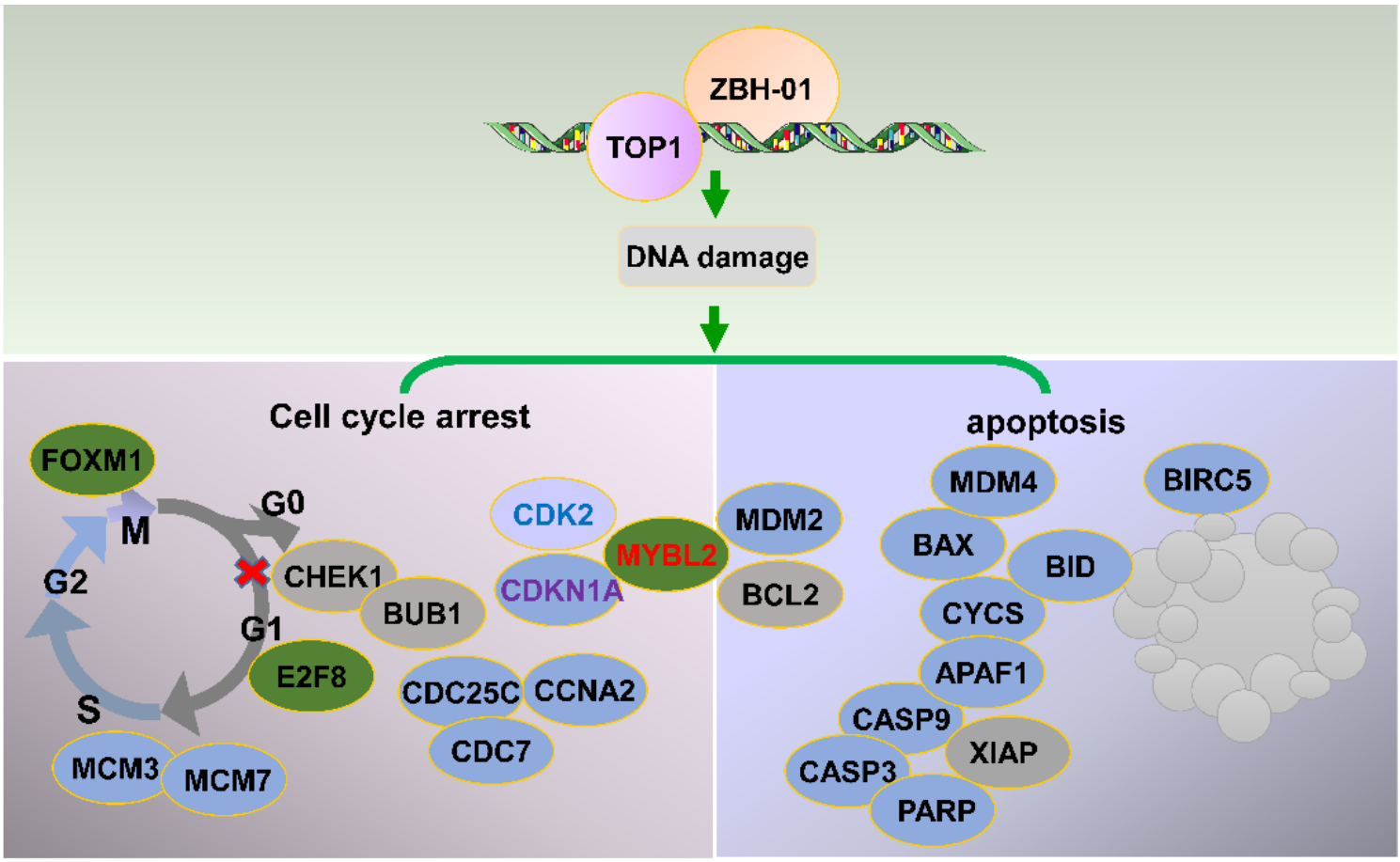

Figure 11

Hypothetical ZBH-01 mechanisms. The DNA damage caused by ZBH-01 induces not only cell cycle arrest but also apoptosis. CCNA2, CDK2, MYBL2, CHEK1, BAX, BCL2L1, caspase 3, and other genes might be regulated by ZBH-01 during cell cycle arrest and apoptosis.